



CHORUS

This is the accepted manuscript made available via CHORUS. The article has been published as:

Steady-state atom-light entanglement with engineered spin-orbit coupling

Meng Wang, Pierre Meystre, Wei Zhang, and Qiongyi He

Phys. Rev. A **93**, 042311 — Published 8 April 2016

DOI: [10.1103/PhysRevA.93.042311](https://doi.org/10.1103/PhysRevA.93.042311)

Steady-state atom-light entanglement with engineered spin-orbit coupling

Meng Wang,¹ Pierre Meystre,² Wei Zhang,^{3,4} and Qiongyi He¹

¹*State Key Laboratory of Mesoscopic Physics, School of Physics, Peking University, Collaborative Innovation Center of Quantum Matter, Beijing 100871, China*

²*Department of Physics and College of Optical Sciences, University of Arizona, Tucson, AZ 85721, USA*

³*Department of Physics, Renmin University of China, Beijing 100872, China*

⁴*Beijing Key Laboratory of Opto-electronic Functional Materials and Micro-nano Devices, Renmin University of China, Beijing 100872, China*

By driving a Bose-Einstein condensate trapped in a single-mode high- Q optical resonator and coupled to a classical transverse running-wave field above a Dicke-like superradiant phase transition, the resulting cavity field-induced spin-orbit coupling leads to a band structure with doubly-degenerate ground states. We show theoretically that the effective bosonic mode defined by interstate hopping can be entangled with the cavity field via the combined effect of spin-orbit coupling and dissipation.

I. INTRODUCTION

Ultracold atomic and molecular systems trapped in optical lattices or in high- Q optical cavities have been at the center of a number of important advances at the interface between atomic, molecular, and optical science and condensed matter physics [1]. Major milestones include the study of the superfluid to Mott insulator quantum phase transition [2, 3], cavity cooling of atoms and molecules [4–6], optical and matter-wave superradiance including transitions from a Mott insulator-like state to a self-ordered superradiant atomic state [7, 8], quantum optomechanical effects including measurements beyond the standard quantum limit [9–11], the development of atom microscopy [12–14], and more. In a recent development, engineered optically induced spin-orbit coupling [15] has been exploited to generate quantum phase transitions [16] and artificial low-dimensional systems that are particularly well suited to study topological effects in many-body systems [17–19].

In parallel work, the importance of robust realizations of quantum entanglement for potential applications in the field of quantum information science [20, 21] has lead to a number of theoretical proposals and experimental demonstrations. Truly macroscopic systems remain however a major challenge due to the increasing rate of environment-induced decoherence [22, 23]. In this context, schemes that exploit quantum dissipation and reservoir engineering for the generation of target quantum states have received increased attention, as they benefit from the double advantage of being independent of specific initial states and of leading to steady states robust against decoherence [24–29].

This paper proposes and analyzes a scheme that combines the effects of engineered spin-orbit coupling and cavity dissipation to achieve a high level of steady-state entanglement between an optical field and a matter wave in a Bose-Einstein condensate (BEC) trapped inside a high- Q optical resonator. The specific atomic system that we consider is characterized by two degenerate hyperfine ground states that are dipole-coupled off-resonantly to a single-mode quantized cavity field as

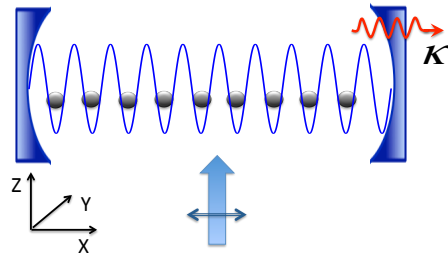


Figure 1. (Color online) A Bose-Einstein condensate trapped inside a Fabry-Pérot resonator with damping rate κ is driven by an off-resonant classical field impinging the atoms from the side of the cavity and a single intracavity mode. These two fields drive a Raman-like transition that couples two hyperfine ground states in a spatially dependent fashion, resulting in spin-orbit coupling in the atoms.

well as to a classical running-wave optical field propagating transversally to the cavity axis, see Fig. 1. These fields drive a Raman transition between the two hyperfine ground states, resulting in an effective spin-orbit coupling (SOC) when photon recoil is also accounted for.

We proceed by first introducing the model, establish the notation, and show how the Raman coupling of the atoms to the two optical fields results in an effective spin-orbit interaction. Decomposing the quantized intracavity field into the sum of a spatially periodic mean field of amplitude α and fluctuations we then study the dependence of the atomic ground state on α only. We show that as a result of the engineered spin-orbit coupling the band structure of the atomic system exhibits two degenerate ground states in the lowest band, one at the center and the other at the edge of the first Brillouin zone, instead of a single minimum as would otherwise be the case. To lowest order the atomic ensemble can therefore be approximated as an effective two-mode bosonic system for which we predict the onset of a Dicke-like phase transition [7, 30–32]. It is characterized by a threshold above which the transverse pumping results in the appearance of a macroscopic population of the intracavity field mode.

We then turn to the effect of the fluctuations. In the limit of a Holstein-Primakoff description of the atomic

modes we find that the atom-field system can be described in terms of a simple two-mode effective Hamiltonian that consist of the sum of a ‘beam-splitter’ and a ‘parametric amplification’ term. When combined with the effects of dissipation this results in the onset of steady-state entanglement between the atoms and the intracavity field. We conclude by exploiting these results to evaluate the entanglement between the matter-wave mode and intracavity optical field.

II. MODEL AND MEAN FIELD ATOMIC GROUND STATE

We consider an atomic BEC trapped inside a high- Q Fabry-Pérot resonator. The atoms are assumed to have two degenerate hyperfine ground levels, and the trap is taken to be sufficiently tight in directions transverse to the cavity axis x that one can restrict the description of their center-of-mass motion to one dimension along that axis. The atoms are coupled off-resonantly to a single quantized cavity mode of frequency ω_0 and wave vector k_0 as well as to a classical plane-wave optical field of frequency ω_A propagating transversally to x , see Fig. 1. These two fields combine to couple the two hyperfine ground states through a Raman-like transition. For far-off resonant excitation the upper electronic level remains essentially unpopulated. Adiabatically eliminating that state in a standard fashion results in the model Hamiltonian ($\hbar = 1$) [33]

$$\begin{aligned} \hat{H} = & \sum_{\sigma} \int dx \hat{\Psi}_{\sigma}^{\dagger}(x) \left[\frac{p_x^2}{2m} + \xi \hat{a}^{\dagger} \hat{a} \cos^2(k_0 x) \right] \hat{\Psi}_{\sigma}(x) \\ & + \eta (\hat{a}^{\dagger} + \hat{a}) \int dx [\hat{\Psi}_{\uparrow}^{\dagger}(x) \cos(k_0 x) \hat{\Psi}_{\downarrow}(x) + \text{h.c.}] \\ & - \Delta_A \hat{a}^{\dagger} \hat{a}, \end{aligned} \quad (1)$$

which is the starting point of our analysis. Here $\hat{\Psi}_{\sigma}(x)$ ($\sigma = \uparrow, \downarrow$) are the annihilation operators for the two hyperfine states, \hat{a} is the annihilation operator for the optical cavity mode, $p_x^2/2m$ is the kinetic energy of the atoms of mass m , and $\xi = g^2/\delta$, with g the vacuum Rabi frequency and δ the detuning between the cavity mode and the atomic transition frequency, is the off-resonant vacuum Rabi frequency between the atoms and the cavity mode. It can be interpreted as the depth of the lattice potential induced by the vacuum cavity field and accounts for the atom-induced dispersive shift of the cavity resonance frequency. The spatial integral is over the length L of the resonator. The second term is an effective spin-orbit coupling contribution that results from the coherent scattering between the transverse pump field and the cavity mode, with an explicit spatial dependence due to the mode structure of the intracavity field. The prefactor is $\eta = \Omega g/\delta$, where Ω is the effective Rabi frequency of the pump field. Finally the last term of \hat{H} accounts for the pump-cavity mode detuning $\Delta_A = \omega_A - \omega_0$. In addition, the intracavity field and atoms are subject to dissipation

at optical and atomic rates κ and γ described by master equations of the familiar Lindblad form.

Ignoring for now the effects of dissipation, which would result in the appearance of additional δ -correlated quantum noise operator contributions to the operator dynamics, the Heisenberg equation of motion for the annihilation operator \hat{a} of the cavity field mode is

$$\begin{aligned} i \frac{d\hat{a}}{dt} = & \hat{a} \left[\xi \sum_{\sigma} \int dx \hat{\Psi}_{\sigma}^{\dagger}(x) \cos^2(k_0 x) \hat{\Psi}_{\sigma}(x) - \Delta_A \right] \\ & + \eta \int dx \left[\hat{\Psi}_{\uparrow}^{\dagger}(x) \cos(k_0 x) \hat{\Psi}_{\downarrow}(x) + \text{h.c.} \right]. \end{aligned} \quad (2)$$

We decompose that operator in the familiar way into the sum of its expectation value $\alpha(t) = \langle \hat{a}(t) \rangle$ and fluctuations $\delta\hat{a}(t)$ as $\hat{a}(t) = \alpha(t) + \delta\hat{a}(t)$. For a constant transverse pump field amplitude η , dissipation at rate κ drives $\alpha(t)$ toward the steady state value

$$\alpha = - \frac{\eta [\int dx \Psi_{\uparrow}^*(x) \cos(k_0 x) \Psi_{\downarrow}(x) + \text{h.c.}]}{\xi \sum_{\sigma} \int dx \Psi_{\sigma}^*(x) \cos^2(k_0 x) \Psi_{\sigma}(x) - \Delta_A - i\kappa}, \quad (3)$$

where we have introduced the expectation values $\Psi_{\sigma} = \langle \hat{\Psi}_{\sigma}(x) \rangle$ of the matter wave field. This permits to express the Hamiltonian that describes the atomic dynamics and optical field fluctuations as the sum of a contribution \hat{H}_1 that accounts for the effects of the classical field α and a term \hat{H}_2 that describes the effects of the field fluctuations as $\hat{H} = \hat{H}_1 + \hat{H}_2$. This gives readily

$$\begin{aligned} \hat{H}_1 = & \sum_{\sigma} \int dx \hat{\Psi}_{\sigma}^{\dagger}(x) \left[\frac{p_x^2}{2m} + \xi |\alpha|^2 \cos^2(k_0 x) \right] \hat{\Psi}_{\sigma}(x) \\ & + \eta (\alpha + \alpha^*) \int dx [\hat{\Psi}_{\uparrow}^{\dagger}(x) \cos(k_0 x) \hat{\Psi}_{\downarrow}(x) + \text{h.c.}] \\ & - \Delta_A |\alpha|^2, \end{aligned} \quad (4)$$

and

$$\begin{aligned} \hat{H}_2 = & (\alpha \delta\hat{a}^{\dagger} + \alpha^* \delta\hat{a} + \delta\hat{a}^{\dagger} \delta\hat{a}) \\ & \times \left[\xi \sum_{\sigma} \int dx \hat{\Psi}_{\sigma}^{\dagger}(x) \cos^2(k_0 x) \hat{\Psi}_{\sigma}(x) - \Delta_A \right] \\ & + \eta (\delta\hat{a} + \delta\hat{a}^{\dagger}) \left[\int dx \hat{\Psi}_{\uparrow}^{\dagger}(x) \cos(k_0 x) \hat{\Psi}_{\downarrow}(x) + \text{h.c.} \right]. \end{aligned} \quad (5)$$

The single-particle mean-field Hamiltonian associated with \hat{H}_1 can be diagonalized in terms of Bloch wave functions. It is characterized by the presence of two degenerate energy minima located respectively at the center and the edge of the first Brillouin zone, see Fig. 2(a). Importantly, as a result of the spin-orbit coupling the lowest band consists of two helicity branches. This is illustrated in Fig. 2(b), which plots a typical example of the spin-up and spin-down populations of the ground state component at the edge of the first Brillouin zone. In that example this component is dominated by the spin-down hyperfine state.

This feature allows one to express the ground state of the atomic system in terms of a two-component

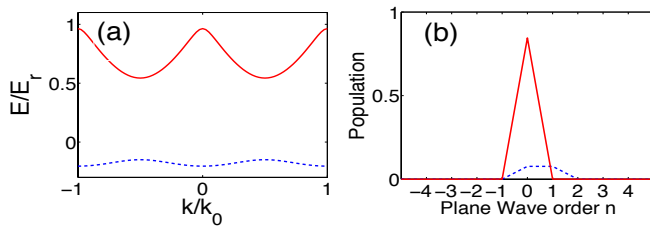


Figure 2. (Color online) (a) Lowest (blue dashed) and first excited (red solid) energy bands of the atomic system. (b) Spin up (blue dashed) and spin down (red solid) populations of the n^{th} plane wave components $\exp(ink_0x)$ of the eigenstate of \hat{H}_1 located at the edge of the first Brillouin zone. Here $\eta = 3$, $\kappa = 1.0 \times 10^4$, $\Delta_A = -1.0 \times 10^4$, $\xi = 1.0$ and $N = 3000$. The energies are scaled to the recoil energy $E_r = k_0^2/2m$.

Schrödinger field $\hat{\Psi}_{\sigma=\uparrow,\downarrow}(x)$, that is a superposition of the bosonic modes associated with the energy minima at the center and the edge of the first Brillouin zone and are characterized by the annihilation operators \hat{C}_1 and \hat{C}_2 , respectively,

$$\hat{\Psi}_{\sigma}(x) = u_{\sigma}\phi_1(x)\hat{C}_1 + v_{\sigma}\phi_2(x)\hat{C}_2. \quad (6)$$

Here $\phi_{1,2}(x)$ are the corresponding Bloch wavefunctions, expanded in the following in terms of a superposition of plane waves $\exp(ink_0x)$ with n integers.

Diagonalizing the mean-field Hamiltonian \hat{H}_1 with the self-consistent expression (3) for the classical cavity field amplitude yields the steady-state solution α for a given transverse pumping strength η as

$$\alpha = -\frac{\eta[\gamma_1|C_1|^2 + \gamma_2|C_2|^2 + (\gamma_3C_1^*C_2 + \text{c.c.})]}{\xi[\lambda_1|C_1|^2 + \lambda_2|C_2|^2 + (\lambda_3C_1^*C_2 + \text{c.c.})] - \Delta_A - i\kappa}, \quad (7)$$

where $C_i = \langle \hat{C}_i \rangle$, c.c. stands for complex conjugate, and

$$\begin{aligned} \lambda_1 &= \int dx |\phi_1(x)|^2 \cos^2(k_0x) (|u_{\uparrow}|^2 + |u_{\downarrow}|^2), \\ \lambda_2 &= \int dx |\phi_2(x)|^2 \cos^2(k_0x) (|v_{\uparrow}|^2 + |v_{\downarrow}|^2), \\ \lambda_3 &= \int dx \phi_1^*(x)\phi_2(x) \cos^2(k_0x) (u_{\uparrow}^*v_{\uparrow} + u_{\downarrow}^*v_{\downarrow}), \\ \gamma_1 &= \int dx |\phi_1(x)|^2 \cos(k_0x) (u_{\uparrow}^*u_{\downarrow} + u_{\downarrow}^*u_{\uparrow}), \\ \gamma_2 &= \int dx |\phi_2(x)|^2 \cos(k_0x) (v_{\uparrow}^*v_{\downarrow} + v_{\downarrow}^*v_{\uparrow}), \\ \gamma_3 &= \int dx \phi_1^*(x)\phi_2(x) \cos(k_0x) (u_{\uparrow}^*v_{\downarrow} + u_{\downarrow}^*v_{\uparrow}). \end{aligned} \quad (8)$$

$$\begin{aligned} \hat{H} &= [(E_2 - E_1) + (\Lambda_2 - \Lambda_1)\delta\hat{a}^\dagger + (\Lambda_2^* - \Lambda_1^*)\delta\hat{a} + \xi(\lambda_2 - \lambda_1)\delta\hat{a}^\dagger\delta\hat{a}] \hat{J}_z + [\xi\hat{N}(\lambda_1 + \lambda_2)/2 - \Delta_A]\delta\hat{a}^\dagger\delta\hat{a} \\ &+ \left\{ [\Lambda_3\delta\hat{a}^\dagger + \Lambda_4^*\delta\hat{a} + \xi\lambda_3\delta\hat{a}^\dagger\delta\hat{a}]\hat{J}_- + [\hat{N}(\Lambda_1 + \Lambda_2)/2 - \Delta_A\alpha]\delta\hat{a}^\dagger + \text{h.c.} \right\} + \hat{N}(E_1 + E_2)/2 - \Delta_A|\alpha|^2, \end{aligned} \quad (9)$$

where $E_1 = E_2$ are the energies of the two degenerate ground states of \hat{H}_1 [35], $\hat{N} = \hat{C}_1^\dagger\hat{C}_1 + \hat{C}_2^\dagger\hat{C}_2$, $\Lambda_1 = \xi\alpha\lambda_1 +$

Figure 3 shows the resulting dependence of $|\alpha|$ on η . It illustrates the onset of a superradiant-like phase transition, with a macroscopic value of the intracavity field amplitude α above a threshold value $\eta_{\text{th}} \approx 2.8$ for the parameters of the figure.

A Dicke-like quantum phase transition in a BEC coupled to an optical cavity and driven by a *standing wave*

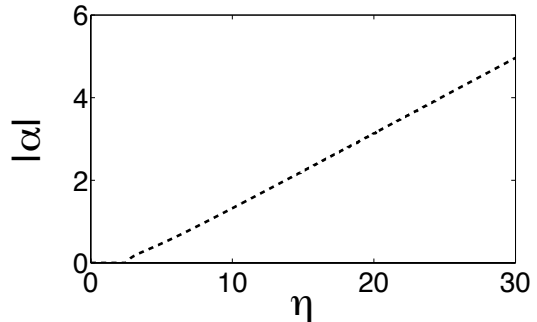


Figure 3. Mean-field intracavity field amplitude $|\alpha|$ as a function of η , illustrating the onset of a Dicke-like phase transition. Same parameters as in Fig. 2.

transverse classical field was observed in an experiment by Baumann *et al.* [7, 34]. The onset of the transition was interpreted in terms of a transition from the suppression of the scattered field inside the cavity mode as a result of destructive interferences from the individual atoms to a situation where the atoms self-organize, thereby maximizing cooperative scattering into the cavity. An analogy between this situation and the original Dicke model [30] was drawn via a two-mode description of the atomic system. A similar mapping is at the origin of the phase transition encountered here, with the difference that instead of using a standing wave driving field, we now have a running wave driving field, and the two-mode description of the atomic systems results from an engineered spin-orbit coupling. Also, in contrast to Ref. [7] we restrict the atomic motion to one dimension instead of two.

III. QUANTUM FLUCTUATIONS

We now turn to a discussion of the quantum fluctuations of the system. Substituting the ground state expression (6) for the matter-wave field operator $\hat{\Psi}_{\sigma}(x)$ into the Hamiltonians \hat{H}_1 and \hat{H}_2 and introducing the angular momentum operators $\hat{J}_+ = \hat{C}_2^\dagger\hat{C}_1$, $\hat{J}_- = \hat{C}_1^\dagger\hat{C}_2$, $\hat{J}_z = (\hat{C}_2^\dagger\hat{C}_2 - \hat{C}_1^\dagger\hat{C}_1)/2$, the Hamiltonian $\hat{H} = \hat{H}_1 + \hat{H}_2$ becomes

$\eta\gamma_1$, $\Lambda_2 = \xi\alpha\lambda_2 + \eta\gamma_2$, $\Lambda_3 = \xi\alpha\lambda_3 + \eta\gamma_3$, and $\Lambda_4 =$

$\xi\alpha\lambda_3^* + \eta\gamma_3^*$.

Next we introduce a Holstein-Primakoff transformation to approximately map the angular momentum operators in Eq. (9) to bosonic annihilation and creation operators \hat{b} and \hat{b}^\dagger , with $\hat{J}_+ = \hat{b}^\dagger\sqrt{N - \hat{b}^\dagger\hat{b}}$, $\hat{J}_- = \hat{J}_+^\dagger$, $\hat{J}_z = \hat{b}^\dagger\hat{b} - N/2$ and $N = \langle \hat{N} \rangle$. Substituting these definitions into Eq. (9) yields

$$\begin{aligned} \hat{H} = & \{[(\Lambda_2 - \Lambda_1)\delta\hat{a}^\dagger + \text{h.c.}] + \xi(\lambda_2 - \lambda_1)\delta\hat{a}^\dagger\delta\hat{a}\}\hat{b}^\dagger\hat{b} \\ & + [\sqrt{N}(\Lambda_3\delta\hat{a}^\dagger + \Lambda_4^*\delta\hat{a} + \xi\lambda_3\delta\hat{a}^\dagger\delta\hat{a})\hat{b} + \text{h.c.}] \\ & + [(N\Lambda_1 - \Delta_A\alpha)\delta\hat{a}^\dagger + \text{h.c.}] + (N\xi\lambda_1 - \Delta_A)\delta\hat{a}^\dagger\delta\hat{a} \\ & + (E_2 - E_1)\hat{b}^\dagger\hat{b} + NE_1 - \Delta_A|\alpha|^2, \end{aligned} \quad (10)$$

where we have kept terms up to quadratic order in \hat{b} and \hat{b}^\dagger only, assuming consistently with the condition of validity of the Holstein-Primakoff approximation that the expectation values of \hat{b} and \hat{b}^\dagger are small in comparison to \sqrt{N} . In the underlying system of a two-component BEC, this corresponds to the case of an attractive effective interaction between two hyperfine spin states, such that all atoms accumulate in one of the two ground states \hat{C}_1 or \hat{C}_2 , leaving the other one almost empty. This is a realistic assumption for the hyperfine manifolds used in most experiments where attractive effective interactions can easily be obtained, e.g. by exploiting the background interaction between atoms. For $N \rightarrow \infty$, the Hamiltonian (10) reduces then to

$$\hat{H}_{\text{eff}} = \omega_a\delta\hat{a}^\dagger\delta\hat{a} + \omega_b\delta\hat{b}^\dagger\delta\hat{b} + [g_1\delta\hat{a}^\dagger\delta\hat{b}^\dagger + g_2\delta\hat{a}^\dagger\delta\hat{b} + \text{h.c.}], \quad (11)$$

where $\omega_a = \xi N\lambda_1 - \Delta_A$, $\omega_b = E_2 - E_1 = 0$, $g_1 = \sqrt{N}\Lambda_4$, $g_2 = \sqrt{N}\Lambda_3$, and $\delta\hat{b}$ is the fluctuation part of mode \hat{b} .

The effective Hamiltonian \hat{H}_{eff} has the form of the linearized quantum optomechanics Hamiltonian [36, 37], with the terms proportional to g_1 and g_2 corresponding to the familiar parametric and beam-splitter interaction, respectively. From the definitions of Λ_3 and Λ_4 it follows that $|g_1| = |g_2|$ grows linearly with η since α also grows almost linearly with η above the transition point η_{th} . The Heisenberg-Langevin equations of motion of the two modes, accounting also for the dissipation of the optical and atomic field at rates κ and γ , and their solution are given in Appendix A.

\hat{H}_{eff} has previously been studied primarily in the near-resonant case $\omega_a = \pm\omega_b$. Here we concentrate instead on the far-off-resonant limit, where the energy of the $\delta\hat{b}$ mode is zero due to the degeneracy of the two ground atomic modes. We investigate the conditions under which this system exhibits quantum entanglement between the optical and matter-wave fields, quantifying it in terms of the logarithmic negativity E_N [38, 39] as defined in Appendix B.

Figure 4(a) shows the dependence of the logarithmic negativity on the ratio γ/κ of the atomic and optical decay rates for several values of the transverse field coupling strength η . It illustrates the existence of a threshold value $(\gamma/\kappa)_{\text{th}}$ below which no entanglement occurs, see

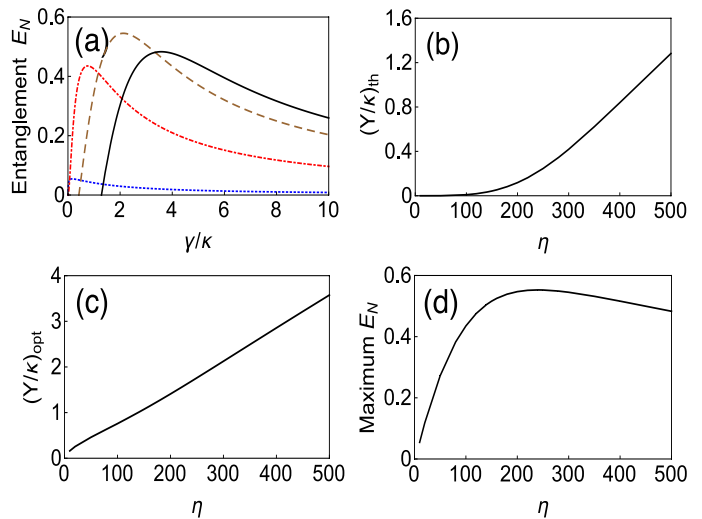


Figure 4. (a) Logarithmic negativity E_N as a function of the normalized decay rate of the atomic mode γ/κ for $\eta = 10$ (blue dotted), $\eta = 100$ (red dot-dashed), $\eta = 300$ (brown dashed), and $\eta = 500$ (black solid). (b) Threshold value $(\gamma/\kappa)_{\text{th}}$ as a function of η . (c) Ratio γ/κ yielding the maximal logarithmic negativity as a function of η . (d) Maximum logarithmic negativity as a function of η . Same parameters as in Fig. 2, and the equilibrium mean thermal excitation numbers of the cavity field and atomic mode are assumed to be zero, $n_{a,\text{in}} = n_{b,\text{in}} = 0$.

Fig. 4(b). Interestingly $(\gamma/\kappa)_{\text{th}}$ increases monotonically with η , a counter-intuitive result that shows the importance of decoherence in balancing the classical driving of the system to achieve quantum entanglement. Figure 4(c) shows the value $(\gamma/\kappa)_{\text{opt}}$ of γ/κ as a function of η , at which the maximum entanglement is obtained, as shown in Fig. 4(d).

IV. SUMMARY AND OUTLOOK

In this paper we have considered a one-dimensional model of a BEC confined to a high- Q optical resonator and driven by a running-wave classical field propagating transversally to the cavity axis, and consequently subject to the combined effects of an engineered spin-orbit coupling interaction and dissipation. This results in the description of the atomic ground state as a degenerate two-mode system that can be mapped to a Dicke-like model. A Holstein-Primakoff description of the system fluctuations further maps it into the linearized Hamiltonian of quantum optomechanics, with both a beam-splitter and parametric coupling components to its dynamics. Combined with the effect of dissipation this results in steady-state quantum entanglement between the matter wave field and optical cavity mode.

This system should be within the reach of state-of-the-art ultracold atomic physics experiments. Quasi-one-dimensional Bose gases can be prepared by trapping

an atomic sample in a two-dimensional lattice potential with tight transverse confinement, leading to an array of quasi-one-dimensional atomic gases with large numbers of atoms. Low optical field dissipation rates κ , of the order of a few MHz, can be achieved in high- Q optical cavities, and the pump parameter η can be easily varied by changing the Rabi frequency Ω of the transvers pump field. As we have seen, it is important that it is comparable to the atomic dissipation rate γ , but this can be controlled by adjusting the collisional loss rate with the density of atoms. Future work will extend this study to a two-dimensional description of the condensate dynamics and many-body effects of the atomic ensemble.

ACKNOWLEDGMENTS

P.M. and M.W. were supported in part by the US Army Research Office. Q.H. acknowledges the support of the National Natural Science Foundation of China under Grants No. 11274025 and No. 61475006. W.Z. acknowledges the support of the National Key Basic Research Program of China under Grant No. 2013CB922000, the National Natural Science Foundation of China under Grant No. 11274009, 11434011, and 11522436, and the Research Funds of Renmin University of China under Grant No. 10XNL016 and 16XNLQ03.

Appendix A: Heisenberg-Langevin equations

Accounting for the dissipation of the optical and atomic field at rates κ and γ and the associated noise operators \hat{a}_{in} and \hat{b}_{in} the Heisenberg-Langevin equations of $\delta\hat{a}$ and $\delta\hat{b}$ are

$$\begin{aligned} \frac{d\delta\hat{a}}{dt} &= -(\kappa + i\omega_a)\delta\hat{a} - ig_2\delta\hat{b} - ig_1\delta\hat{b}^\dagger - \sqrt{2\kappa}\hat{a}_{\text{in}}, \\ \frac{d\delta\hat{b}}{dt} &= -(\gamma + i\omega_b)\delta\hat{b} - ig_2^*\delta\hat{a} - ig_1\delta\hat{a}^\dagger - \sqrt{2\gamma}\hat{b}_{\text{in}}, \end{aligned} \quad (\text{A1})$$

where as usual the noise operators \hat{a}_{in} and \hat{b}_{in} are assumed to be δ -correlated,

$$\begin{aligned} \langle \hat{a}_{\text{in}}(t)\hat{a}_{\text{in}}^\dagger(t') \rangle &= (n_{a,\text{in}} + 1)\delta(t - t'), \\ \langle \hat{b}_{\text{in}}(t)\hat{b}_{\text{in}}^\dagger(t') \rangle &= (n_{b,\text{in}} + 1)\delta(t - t'), \end{aligned} \quad (\text{A2})$$

and $n_{a,\text{in}}$ and $n_{b,\text{in}}$ are the mean thermal excitations of modes $\delta\hat{a}$ and $\delta\hat{b}$, respectively. Introducing further the quadrature operators

$$\begin{aligned} \hat{X}_a &= (\delta\hat{a} + \delta\hat{a}^\dagger)/\sqrt{2}, \\ \hat{P}_a &= (\delta\hat{a} - \delta\hat{a}^\dagger)/(\sqrt{2}i), \end{aligned} \quad (\text{A3})$$

and similarly for the atomic field, and with the compact notation

$$\begin{aligned} \hat{u}(t) &= [\hat{X}_a, \hat{P}_a, \hat{X}_b, \hat{P}_b]^T, \\ \hat{n}(t) &= -[\sqrt{2\kappa}\hat{X}_{\text{in},a}, \sqrt{2\kappa}\hat{P}_{\text{in},a}, \sqrt{2\gamma}\hat{X}_{\text{in},b}, \sqrt{2\gamma}\hat{P}_{\text{in},b}]^T, \end{aligned}$$

we find

$$\frac{d\hat{u}}{dt} = \mathbf{A}\hat{u}(t) + \hat{n}(t), \quad (\text{A4})$$

where

$$\mathbf{A} = \begin{bmatrix} -\kappa & \omega_a & \text{Im } g & -\text{Re } g' \\ -\omega_a & -\kappa & -\text{Re } g & -\text{Im } g' \\ \text{Im } g' & -\text{Re } g' & -\gamma & \omega_b \\ -\text{Re } g & -\text{Im } g & -\omega_b & -\gamma \end{bmatrix}. \quad (\text{A5})$$

Here, the coefficients are $g = g_1 + g_2$ and $g' = g_1 - g_2$. The formal solution of Eq. (A4) is

$$\hat{u}(t) = \exp(\mathbf{A}t)\hat{u}(0) + \int_0^t \exp(\mathbf{A}t')\hat{n}(t-t')dt'. \quad (\text{A6})$$

According to the Routh-Hurwitz criterion, the system is stable if all eigenvalues of the matrix \mathbf{A} have a negative real part, in which case $\exp(\mathbf{A}t) \rightarrow 0$ for $t \rightarrow \infty$ so that

$$\hat{u}(\infty) = \lim_{t \rightarrow \infty} \int_0^t \exp(\mathbf{A}t')\hat{n}(t-t')dt'. \quad (\text{A7})$$

Appendix B: Atom-field entanglement

The atom-field entanglement can be quantified in terms of the logarithmic negativity [38, 39]

$$E_N = \max\{0, -\log_2[2\eta^-]\}, \quad (\text{B1})$$

where

$$\eta^- = \frac{1}{\sqrt{2}}\sqrt{\sigma - \sqrt{[\sigma^2 - 4\det \mathbf{V}]}}, \quad (\text{B2})$$

$$\sigma = \det \mathbf{V}_a + \det \mathbf{V}_b - 2\det \mathbf{V}_{ab}, \quad (\text{B3})$$

and \mathbf{V}_a and \mathbf{V}_{ab} are the sub-matrices of the 2×2 block form

$$\mathbf{V} = \begin{bmatrix} \mathbf{V}_a & \mathbf{V}_{ab} \\ \mathbf{V}_{ab}^T & \mathbf{V}_b \end{bmatrix} \quad (\text{B4})$$

of the covariance matrix \mathbf{V} with matrix elements

$$V_{ij} = \frac{1}{2}\langle \hat{u}_i(\infty)\hat{u}_j(\infty) + \hat{u}_j(\infty)\hat{u}_i(\infty) \rangle - \langle \hat{u}_i(\infty) \rangle \langle \hat{u}_j(\infty) \rangle. \quad (\text{B5})$$

The covariance matrix can be obtained from Eq. (A7), which yields the Lyapunov equation [40]

$$\mathbf{A}\mathbf{V} + \mathbf{V}\mathbf{A}^T = -\mathbf{D}, \quad (\text{B6})$$

where the matrix \mathbf{D} is given by

$$\mathbf{D} = \text{diag} \left\{ 2\kappa\Delta^2\hat{X}_{\text{in},a}, 2\kappa\Delta^2\hat{P}_{\text{in},a}, 2\gamma\delta^2\hat{X}_{\text{in},b}, 2\gamma\Delta^2\hat{P}_{\text{in},b} \right\} \quad (\text{B7})$$

and $\Delta^2\hat{O} \equiv \langle \hat{O}^2 \rangle - \langle \hat{O} \rangle^2$ is the variance of the operator \hat{O} .

- [1] M. Lewenstein, A. Sanpera, and V. Ahufinger, *Ultracold atoms in optical lattices*, Oxford University Press, Oxford, U.K. (2012).
- [2] D. Jaksch, C. Bruder, J. I. Cirac, C. W. Gardiner, and P. Zoller, Cold bosonic atoms in optical lattices, *Phys. Rev. Lett.* **81**, 3108 (1998).
- [3] M. Greiner, O. Mandel, T. Esslinger, T. W. Hänsch, and I. Bloch, Quantum phase transition from a superfluid to a Mott insulator in a gas of ultracold atoms. *Nature* **415**, 39 (2001).
- [4] P. Horak, G. Hechenblaikner, K. M. Gheri, H. Stecher, and H. Ritsch, Cavity-induced atom cooling in the strong coupling regime, *Phys. Rev. Lett.* **79**, 4974 (1997).
- [5] V. Vuletic and S. Chu, Laser cooling of atoms, ions, or molecules by coherent scattering, *Phys. Rev. Lett.* **84**, 3787 (2000).
- [6] P. Maunz, T. Puppe, I. Schuster, N. Syassen, P. W. H. Pinkse, and G. Rempe, Cavity cooling of a single atom, *Nature* **428**, 50 (2004).
- [7] K. Baumann, C. Guerlin, F. Brennecke, and T. Esslinger, Dicke quantum phase transition with a superfluid gas in an optical cavity, *Nature* **464**, 1301 (2010).
- [8] H. Ritsch, P. Domokos, F. Brennecke, and T. Esslinger, Cold atoms in cavity-generated dynamical optical potentials, *Rev. Mod. Phys.* **85**, 553 (2013).
- [9] D. Teufel, T. Donner, M. A. Castellanos-Beltran, J. W. Harlow, and K. W. Lehnert, Nanomechanical motion measured with an imprecision below that at the standard quantum limit, *Nature Nanotech.* **4**, 820 (2009).
- [10] G. Anetsberger, O. Arcizet, Q. P. Unterreithmeier, R. Rivière, A. Schliesser, E. M. Weig, J. P. Kotthaus, and T. J. Kippenberg, Near-field cavity optomechanics with nanomechanical oscillators, *Nature Phys.* **5**, 909 (2009).
- [11] S. Schreppler, N. Spethmann, N. Brahms, T. Botter, M. Barrios, and D. M. Stamper-Kurn, Optically measuring force near the standard quantum limit, *Science* **344**, 1486 (2014).
- [12] W. S. Bakr, J. I. Gillen, A. Peng, S. Fölling, M. Greiner, A Quantum Gas Microscope for detecting single atoms in a Hubbard regime optical lattice, *Nature* **462**, 74-77 (2009).
- [13] W. S. Bakr, A. Peng, M. E. Tai, R. Ma, J. Simon, J. I. Gillen, S. Fölling, L. Pollet, and M. Greiner, Probing the Superfluid to Mott Insulator Transition at the Single-Atom Level, *Science* **329**, 547 (2010).
- [14] C. Weitenberg, M. Endres, J. F. Sherson, M. Cheneau, P. Schau, T. Fukuhara, I. Bloch, and S. Kuhr, Single-spin addressing in an atomic Mott insulator, *Nature* **471**, 319 (2011).
- [15] X.-J. Liu, M. F. Borunda, Xin Liu, and J. Sinova, Effect of induced spin-orbit coupling for atoms via laser fields, *Phys. Rev. Lett.* **102**, 046402 (2009).
- [16] Y. J. Lin, K. Jimenez-Garcia, and I. B. Spielman, Spin-orbit-coupled Bose-Einstein condensates, *Nature* **471**, 83 (2011).
- [17] A. Celi, P. Massignan, J. Ruseckas, N. Goldman, I. B. Spielman, G. Juzeliunas, and M. Lewenstein, Synthetic gauge fields in synthetic dimensions, *Phys. Rev. Lett.* **112**, 043001 (2014).
- [18] B. K. Stuhl, H.-I. Lu, L. M. Aycock, D. Genkina, and I. B. Spielman, Visualizing edge states with an atomic Bose gas in the quantum Hall regime, *Science* **349**, 1514 (2015).
- [19] M. Mancini, G. Pagano, G. Cappellini, L. Livi, M. Rider, J. Catani, C. Sias, P. Zoller, M. Inguscio, M. Dalmonte, and L. Fallani, Observation of chiral edge states with neutral fermions in synthetic Hall ribbons, *Science* **349** (2015).
- [20] S. L. Braunstein and P. van Loock, Quantum information with continuous variables, *Rev. Mod. Phys.* **77**, 513 (2005).
- [21] R. Horodecki, P. Horodecki, M. Horodecki, and K. Horodecki, Quantum entanglement, *Rev. Mod. Phys.* **81**, 865 (2009).
- [22] W. H. Zurek, Decoherence, einselection, and the quantum origins of the classical, *Rev. Mod. Phys.* **75**, 715 (2003).
- [23] T. Monz, P. Schindler, J. T. Barreiro, M. Chwalla, D. Nigg, W. A. Coish, M. Harlander, W. Hänsel, M. Hennrich, and R. Blatt, 14-Qubit Entanglement: Creation and Coherence, *Phys. Rev. Lett.* **106**, 130506 (2011).
- [24] J. T. Barreiro, P. Schindler, O. Guhne, T. Monz, M. Chwalla, C. F. Roos, M. Hennrich, and R. Blatt, Experimental multiparticle entanglement dynamics induced by decoherence, *Nature Phys.* **6**, 943 (2010).
- [25] H. Krauter, C. A. Muschik, K. Jensen, W. Wasilewski, J. M. Petersen, J. I. Cirac, and E. S. Polzik, Entanglement Generated by Dissipation and Steady State Entanglement of Two Macroscopic Objects, *Phys. Rev. Lett.* **107**, 080503 (2011).
- [26] Y. Lin, J. P. Gaebler, F. Reiter, T. R. Tan, R. Bowler, A. S. Sørensen, D. Leibfried, and D. J. Wineland, Dissipative production of a maximally entangled steady state of two quantum bits, *Nature (London)* **504**, 415 (2013).
- [27] A. Bermudez, T. Schaetz, and M. B. Plenio, Dissipation-assisted quantum information processing with trapped ions, *Phys. Rev. Lett.* **110**, 110502 (2013).
- [28] M.J. Kastoryano, F. Reiter, and A. S. Sørensen, Dissipative preparation of entanglement in optical cavities, *Phys. Rev. Lett.* **106**, 090502 (2011).
- [29] A. Metelmann and A. A. Clerk, Nonreciprocal Photon Transmission and Amplification via Reservoir Engineering, *Phys. Rev. X* **5**, 021025 (2015).
- [30] R. H. Dicke, Coherence in spontaneous radiation processes, *Phys. Rev.* **93**, 99 (1954).
- [31] F. Dimer, B. Estienne, A. S. Parkins, and H. J. Carmichael, Proposed realization of the Dicke-model quantum phase transition in an optical cavity QED system, *Phys. Rev. A* **75**, 013804 (2007).
- [32] D. Nagy, G. Konya, G. Szirmai, and P. Domokos, Dicke-model phase transition in the quantum motion of a Bose-Einstein condensate in an optical cavity, *Phys. Rev. Lett.* **104**, 130401 (2010).
- [33] J.-S. Pan, X.-J. Liu, W. Zhang, W. Yi, and G.-C. Guo, Topological Superradiant States in a Degenerate Fermi Gas, *Phys. Rev. Lett.* **115**, 045303 (2015).
- [34] K. G. Baumann, Experimental realization of the Dicke quantum phase transition, ETH Zürich PhD Dissertation No. 19943 (2011).
- [35] Although $E_1 = E_2 \equiv E$ we keep track of the term $E_2 - E_1$ in Eq. (9) to help illustrate the analogy with a more familiar form of an effective Hamiltonian.

- [36] M. Aspelmeyer, T. J. Kippenberg, and F. Marquardt, Cavity optomechanics, *Rev. Mod. Phys.* **86**, 1391 (2014).
- [37] P. Meystre, A short walk through quantum optomechanics, *Annalen der Physik* **525**, 215 (2013).
- [38] G. Vidal and R. F. Werner, Computable measure of entanglement, *Phys. Rev. A* **65**, 032314 (2002).
- [39] G. Adesso, A. Serafini, and F. Illuminati, Extremal entanglement and mixedness in continuous variable systems, *Phys. Rev. A* **70**, 022318 (2004).
- [40] M. Bhattacharya, P.-L. Giscard and P. Meystre, Entanglement of a Laguerre-Gaussian cavity mode with a rotating mirror, *Phys. Rev. A* **77**, 013827 (2008).